Research Article | Vol. 26, No. 2 | 22 Jan 2018 | OPTICS EXPRESS 897
Optics EXPRESS

Improvement in focusing accuracy of DNA sequencing microscope with multi-position laser differential confocal autofocus method

XIN ZHANG,[1,2,*] FEI ZENG,[1,2] YI LI,[1] AND YANFENG QIAO[1]

[1]*Changchun Institute of Optics, Fine Mechanics and Physics, Chinese Academy of Sciences, Changchun 130033, China*
[2]*University of Chinese Academy of Sciences, Beijing 100049, China*
**zhangxin@tju.edu.cn*

Abstract: High focusing accuracy in microscopes could improve the imaging quality to reduce the error rate in DNA sequencing. We propose a new feedback method to improve the focusing condition to a very high accuracy. A reference laser reflected by the sample is detected by two or more sensors around the confocal point. After acquiring the signals from the out-of-focus positions, online data processing is implemented to provide feedbacks for real-time focus-plane locking on the sample surface. This method provides an accuracy better than 1/10 of the objective depth-of-focus. To balance optical aberrations, a specific optical feedback system should be designed, with athermal design considerations to adapt DNA sequencing work to temperature fluctuations.

OCIS codes: (120.0120) Instrumentation, measurement, and metrology; (180.1790) Confocal microscopy.

References and links

1. M. C. Wendl and R. K. Wilson, "Aspects of coverage in medical DNA sequencing," BMC Bioinformatics **9**(12), 239 (2008).
2. F. Haque, J. Li, H. C. Wu, X. J. Liang, and P. Guo, "Solid-state and biological nanopore for real-time sensing of single chemical and sequencing of DNA," Nano Today **8**(1), 56–74 (2013).
3. S. Bhattacharya, J. Yoo, and A. Aksimentiev, "Water Mediates Recognition of DNA Sequence via Ionic Current Blockade in a Biological Nanopore," ACS Nano **10**(4), 4644–4651 (2016).
4. S. J. Lassiter, W. Stryjewski, B. L. Legendre, Jr., R. Erdmann, M. Wahl, J. Wurm, R. Peterson, L. Middendorf, and S. A. Soper, "Time-resolved fluorescence imaging of slab gels for lifetime base-calling in DNA sequencing applications," Anal. Chem. **72**(21), 5373–5382 (2000).
5. E. Viegas-Pequignot, B. Dutrillaux, H. Magdelenat, and M. Coppey-Moisan, "Mapping of single-copy DNA sequences on human chromosomes by in situ hybridization with biotinylated probes: Enhancement of detection sensitivity by intensified-fluorescence digital-imaging microscopy," Proc. Natl. Acad. Sci. U.S.A. **86**(2), 582–586 (1989).
6. P. Latreille, S. Norton, B. S. Goldman, J. Henkhaus, N. Miller, B. Barbazuk, H. B. Bode, C. Darby, Z. Du, S. Forst, S. Gaudriault, B. Goodner, H. Goodrich-Blair, and S. Slater, "Optical mapping as a routine tool for bacterial genome sequence finishing," BMC Genomics **8**(6), 321 (2007).
7. L. F. McKeogh, J. P. Sharpe, and K. M. Johnson, "A low-cost automatic translation and autofocusing system for a microscope," Meas. Sci. Technol. **6**(5), 583–587 (1995).
8. C. Gierl, T. Kondo, H. Voos, W. Kongprawechon, and S. Phoojaruenchanachai, "Image processing algorithms for an auto focus system for slit lamp microscopy," *Advanced Concepts for Intelligent Vision Systems. Proc. Springer* **4678**, 909–919 (2007).
9. R. Nishi, Y. Moriyama, K. Yoshida, N. Kajimura, H. Mogaki, M. Ozawa, and S. Isakozawa, "An autofocus method using quasi-Gaussian fitting of image sharpness in ultra-high-voltage electron microscopy," Microscopy (Oxf.) **62**(5), 515–519 (2013).
10. K. H. Kim, S. Y. Lee, S. Kim, S. H. Lee, and S. G. Jeong, "A new DNA chip detection mechanism using optical pick-up actuators," Microsyst. Technol. **13**(8), 1359–1369 (2007).
11. W. Y. Hsu, C. S. Lee, P. J. Chen, N. T. Chen, F. Z. Chen, Z. R. Yu, C. H. Kuo, and C. H. Hwang, "Development of the fast astigmatic auto-focus microscope system," Meas. Sci. Technol. **20**(4), 045902 (2009).
12. C. S. Liu, Y. C. Lin, and P. H. Hu, "Design and characterization of precise laser-based autofocusing microscope with reduced geometrical fluctuations," Microsyst. Technol. **19**(11), 1717–1724 (2013).
13. J. Yang, L. Qiu, W. Zhao, and H. Wu, "Laser differential reflection-confocal focal-length measurement," Opt. Express **20**(23), 26027–26036 (2012).

#313712 https://doi.org/10.1364/OE.26.000887
Journal © 2018 Received 20 Nov 2017; revised 16 Dec 2017; accepted 17 Dec 2017; published 9 Jan 2018

Optics EXPRESS

14. Z. Li, L. Qiu, W. Zhao, and S. Yang, "Laser differential confocal ultra-large radius measurement for convex spherical surface," Opt. Express **24**(17), 19746–19759 (2016).
15. Z. Li, L. Qiu, W. Zhao, and Q. Zhao, "Laser multi-reflection differential confocal long focal-length measurement," Appl. Opt. **55**(18), 4910–4916 (2016).
16. J. Yang, L. Qiu, W. Zhao, Y. Shen, and H. Jiang, "Laser differential confocal paraboloidal vertex radius measurement," Opt. Lett. **39**(4), 830–833 (2014).
17. R. J. Noll, "Zernike polynomials and atmosphere turbulence," J. Opt. Soc. Am. **66**(3), 207–211 (1976).
18. CODE V Lens System Setup Reference Manual, Version **11**(1), 580–581 (2017) (Synopsys, Inc.).

1. Introduction

DNA sequencing is the process for determining the order of four bases (A, G, C, T), which plays an important role in fields, such as, biological science, medical diagnosis, and agricultural development [1–3]. In recent years, the fluorescence-based microscope imaging method, which makes DNA sequencing easier and faster, has become the most widely used method in DNA sequencing [4,5]. High-quality fluorescence imaging is the urgent requirement for high-throughput DNA sequencing [6]. Imaging quality relies not only on a high-performance microscope but also on precise focal-plane determination, as fast and accurate focusing on the sample surface is needed. High-throughput DNA sequencing processes large amounts of data every day, which means that the time interval for sequentially capturing each image should be as short as possible. In a high-throughput DNA sequencing process, after the imaging of one DNA sample area is completed, which requires an exposure time of the order of tens of milliseconds due to weak DNA fluorescence signal, the next DNA sample area moves to the microscope's field of view quickly. Meanwhile, the autofocus system detects the defocus and sends a signal to the focus motor. This is a closed-loop iteration control process, so that a short defocus detection time is needed for rapid focusing to improve DNA sequencing throughput; moreover, an autofocus accuracy of the order of a quarter of the objective depth-of-focus is needed for diffractive-limited performance to increase the probability of base identification. Therefore, the development of a fast and precise autofocus microscope is imperative.

The commonly used autofocus method for microscopes is based on image processing [7–9]. This method, which rapidly scans the focusing position and identifies the image sharpness, is reliable and robust, and able to obtain a clear image on the accurate focal position. However, each imaging attempt needs tens of milliseconds of exposure time, and image processing is also time-consuming. The closed-loop iteration control process needs multiple-exposure imaging, which will consume more time. Therefore, this method is not suitable for high-throughput DNA sequencing. Fast autofocus microscopes based on photoelectric detection have been developed and utilized [10–12]. The astigmatic autofocus method using a quadrant detector achieves high accuracy, but does not include any analysis of the system aberration or translational displacement. Precise autofocus capability is achieved using a centroid position feedback signal captured by a charge-coupled device (CCD) sensor, whose fast tracking autofocus accuracy is approximately half of the depth-of-focus. These photoelectric detection methods have achieved fast autofocus performances with high accuracy for microscopes, but cannot satisfy the requirements of high-throughput DNA sequencing.

In this paper, an extremely fast and high-accuracy autofocus method for high-throughput DNA sequencing is proposed. By applying the laser differential confocal focusing approach [13] to automatically lock the focal plane of the fluorescence microscope, high-accuracy and fast autofocusing is achieved, which provides an autofocus accuracy better than 1/10 of the objective depth-of-focus. Although ultrahigh accuracy is achieved, the intrinsically small linear range of the laser differential confocal technology limits its applications. Considering the actual requirements of a DNA sequencing microscope, a multi-position laser differential confocal method is proposed in this study to extend the working range up to several times the depth of focus. This method is based on photoelectric detection using a photodiode whose response time is several nanoseconds. The defocusing distance is obtained through real-time

Optics EXPRESS

differential subtraction of the voltage signals within a millisecond using a common processor. Therefore, this autofocus method is suitable for high-throughput DNA sequencing.

2. Principle of laser differential confocal autofocus method

The laser differential confocal method has been extensively applied in the field of precision measurement [14–16]. Here, it is introduced to an autofocus microscope for DNA sequencing. Figure 1 shows the layout of the optical microscope with the proposed laser differential confocal autofocus system. The silicon wafer with a fluorescently tagged DNA segment is located on the focal plane of the microscope. The DNA segment is placed in a patterned array of spots, whose diameter is less than 1 μm. The surface of the silicon wafer reflects light like a mirror, which can be used as an autofocus target. The microscope consists of an infinity-corrected objective and a tube lens. The autofocus system consists of a collimating lens, a single mode fiber (SMF) laser, two pieces of beam-splitters (BS), and a pair of pinholes and photodiodes (PDs). A parallel laser beam is produced by the collimating lens, focused with the microscopy objective, reflected back to the autofocus system by the silicon wafer near the focal plane, split by BS 2 into two components, and finally detected by the PD pair with pinholes before and after the focus.

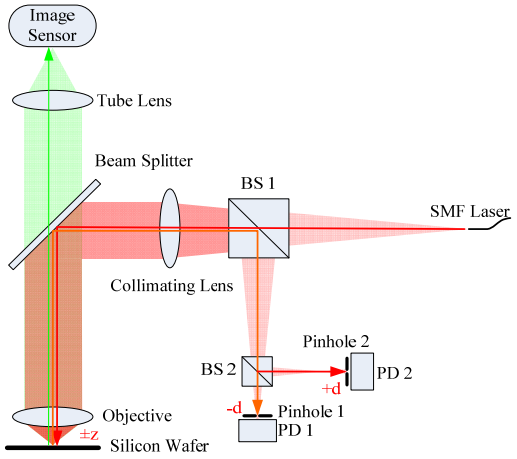

Fig. 1. Microscope with the laser differential confocal autofocus system. BS is the beam splitter, PD is the photodiode, d is the offset distance of the PDs with pinhole from the focus of the collimating lens, z is the defocus distance of the silicon wafer from the focus plane of the microscope objective, and SMF Laser is the laser with single-mode-fiber output.

The response signals of the photodiodes are expressed as I_1 and I_2 for PD 1 and PD 2, respectively. Based on the laser differential confocal principle [13], the differential confocal response signal $I(u_o, u_c)$ obtained through the differential subtraction of I_1 and I_2 can be derived as follows

$$I(u_o,u_c)=I_1-I_2=\left[\frac{\sin(u_o/2-u_c/4)}{u_o/2-u_c/4}\right]^2-\left[\frac{\sin(u_o/2+u_c/4)}{u_o/2+u_c/4}\right]^2 \tag{1}$$

where,

$$u_o=\frac{\pi}{2\lambda}\frac{D^2}{f_o^2}z \tag{2}$$

$$u_c=\frac{\pi}{2\lambda}\frac{D^2}{f_c^2}d \tag{3}$$

Optics EXPRESS

where λ (850 nm) is the wavelength of the collimated laser for probing the focus, D is the diameter of the laser beam, f_o is the focal length of the microscope objective, and f_c is the focal length of the collimating lens.

When $u_o = 0$, the differential confocal signal $I(u_o, u_c) = 0$, and the silicon wafer is exactly on the focal plane. When $u_o \neq 0$, the differential confocal signal $I(u_o, u_c) \neq 0$, and the silicon wafer is out of focus.

From Eq. (2) and (3), we can discern that u_c depends on d, which is the offset of the PDs from the focal plane of the collimating lens, while u_o depends on z, which is the defocus distance of the silicon wafer from the focal plane of the microscope objective.

Figure 2 shows the differential confocal autofocus sensitivity with different u_c. The autofocus system has the largest sensitivity corresponding to the maximum slope of the differential confocal signal curve when $u_c = 5.21$, while it has the maximum working range corresponding to the maximum monotonic region of the differential confocal signal curve when $u_c = 4\pi$.

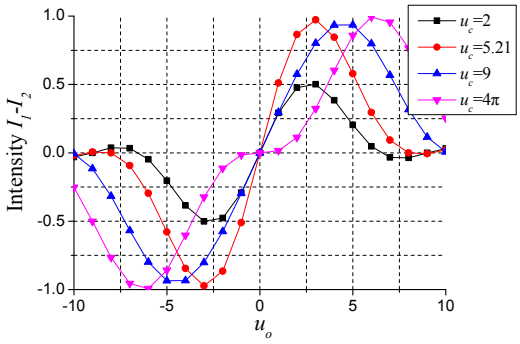

Fig. 2. Differential confocal autofocus sensitivity and monotonic region with different u_c.

To obtain a large sensitivity and a linear working range, u_c should be around 5.21, and the working-range parameter u_o is ± 2.72 according to the autofocus working range.

The pinholes are used as spatial filters to stop the airy disk before and after the focusing, except for a small area near the central point of the airy disk. The effect of the size of the pinholes on the focusing sensitivity is analyzed, which indicates that the normalized radius of the pinholes should be less than 2 [14]. The actual radius of the pinholes is described as follows

$$r_p \le \frac{2\lambda}{\pi(D/f_c)}. \tag{4}$$

The differential confocal position error σ can be described as [13]:

$$\sigma = \frac{2\lambda}{0.54\pi \cdot SNR \cdot (D/f_o)^2}. \tag{5}$$

where SNR is the signal-to-noise ratio of the PDs. The SNR of the PDs is greater than 10. For a series of microscope objectives, which can be used in DNA sequencing, the required parameters and autofocus parameters calculated from Eq. (2) and (5) are listed in Table 1, where the required working range depends on the repetitive positioning accuracy of the object stage, and the required focusing accuracy depends on imaging quality, equal to a quarter of the depth-of-focus.

Optics EXPRESS

Table 1. Required Parameters and Autofocus Parameters for Microscope Objective

	NA = 0.5	NA = 0.75	NA = 1.0
Depth of focus	± 1.2 μm	± 0.53 μm	± 0.3 μm
Required working range	± 1 μm	± 1 μm	± 1 μm
Required focusing accuracy	0.3 μm	0.13 μm	0.075 μm
Autofocus working range	± 1 μm	± 0.46 μm	± 0.37 μm
Autofocus accuracy	0.1 μm	0.045 μm	0.025 μm

This method provides an autofocus accuracy better than 1/10 of the objective depth-of-focus, which can satisfy the requirement of the microscope for DNA sequencing. However, the autofocus working range cannot satisfy the requirement when the numerical aperture (NA) is larger than 0.5. To expand the autofocus working range, a multi-position laser differential confocal autofocus method is proposed in this study.

3. Multi-position laser differential confocal autofocus method

Figure 3 shows the layout of the developed multi-position laser differential confocal autofocus method. Here, four photodiodes with pinholes are respectively placed at the −d, + d, −3d, + 3d positions offset from the focus of the collimating lens.

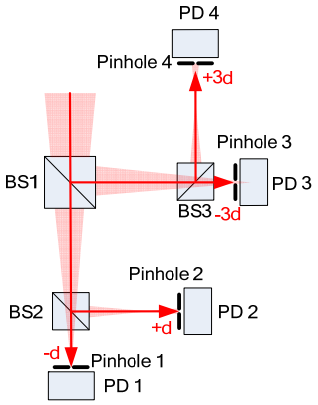

Fig. 3. Layout of the multi-position laser differential confocal autofocus method.

The normalized photodiode-detected signals are denoted as I_1, I_2, I_3, and I_4, as shown in Fig. 4. The largest and the second largest signals among I_1 to I_4 can be used as differential confocal signals, determining the value of u_o, according to different off-focal distances.

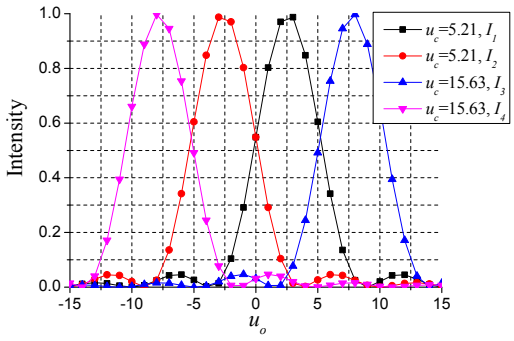

Fig. 4. Normalized detected signals of the multi-position photodiodes.

Then the normalized differential confocal signal can be modified as follows

Optics EXPRESS

$$I(u_o,u_c)=\begin{cases}\left[\dfrac{\sin(u_o/2-3u_c/4)}{u_o/2-3u_c/4}\right]^2-\left[\dfrac{\sin(u_o/2-u_c/4)}{u_o/2-u_c/4}\right]^2 & -8.16<u_o<-2.72\\ \left[\dfrac{\sin(u_o/2-u_c/4)}{u_o/2-u_c/4}\right]^2-\left[\dfrac{\sin(u_o/2+u_c/4)}{u_o/2+u_c/4}\right]^2 & -2.72\le u_o\le 2.72.\\ \left[\dfrac{\sin(u_o/2+u_c/4)}{u_o/2+u_c/4}\right]^2-\left[\dfrac{\sin(u_o/2+3u_c/4)}{u_o/2+3u_c/4}\right]^2 & 2.72<u_o<8.16\end{cases} \quad (6)$$

Figure 5 shows the multi-position laser differential confocal signal curves that have the maximum sensitivity and uniform monotonicity in three regions: $-8.16< u_o <-2.72$, $-2.72\le u_o\le 2.72$ and $2.72<u_o<8.16$. The autofocus working range is expanded to ± 1.38 μm for NA = 0.75 and ± 1.11 μm for NA = 1.0. Referring back to Table 1, apparently, the autofocus working range can satisfy the requirement of the microscope for DNA sequencing.

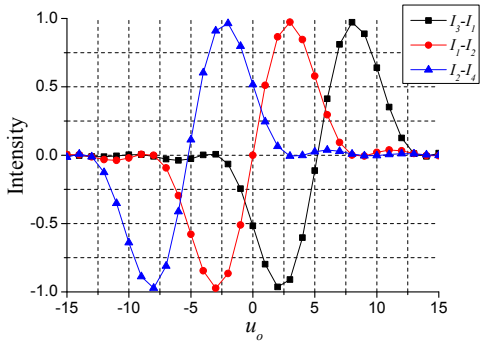

Fig. 5. Multi-position laser differential confocal signal curves.

4. Effect of optical system aberrations on the autofocus

As some aberrations exist in the actual optical system, it is necessary to analyze the effect of the optical system aberrations on the autofocus microscope. Because the laser differential confocal autofocus system works on the optical axis of the microscope objective, theoretically, there is only spherical aberration. However, during the fabrication process, astigmatism and coma are likely to be introduced. The Zernike polynomial coefficients [17] are used to analyze the effects of spherical aberration, astigmatism, and coma. To facilitate the use of computer program analysis, the Fringe Zernike polynomial [18] is used here, which was originally developed at the University of Arizona, and is used in the Fringe program. It is also used by several vendors of interferometers and interferometer software. It has a maximum of 37 terms, which are a subset of the standard Zernike polynomials, arranged in a different order, in which, Z9 is the primary spherical aberration, Z8 is the primary coma, Z5 is the primary astigmatism, and Z4 is the defocus.

Figure 6 shows the rapid decrease in the differential confocal autofocus sensitivity with the increase in spherical aberration, astigmatism, and coma. Compared to coma and astigmatism, spherical aberration is more serious. Moreover, the differential confocal signal is not equal to zero when the silicon wafer is on the focus plane of the microscope objective.

Optics EXPRESS

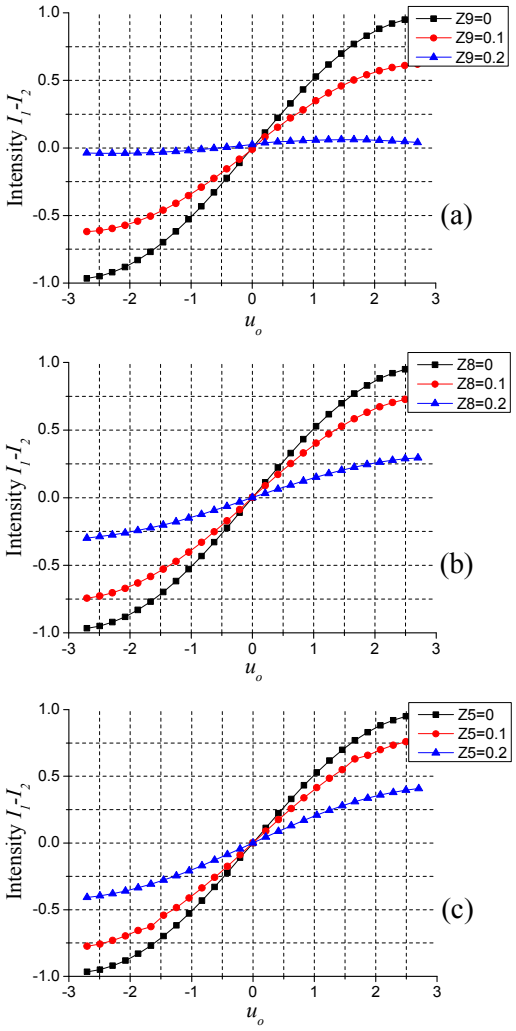

Fig. 6. Rapid decrease in differential confocal autofocus sensitivity with the increase in aberration, (a) spherical aberration (Z9), (b) coma (Z8), and (c) astigmatism (Z5).

To obtain high autofocus sensitivity, the aberrations of the microscope objective with an autofocus system must be as small as possible, especially the spherical aberration. Spherical aberration, as a type of axial symmetric aberration, can be compensated by the collimating lens. In addition, the working wavelength of the microscope for DNA sequencing is from 500 nm to 700 nm, while the wavelength of the laser for probing the focus is 850 nm. Because the autofocus laser wavelength is far away from the fluorescence waveband, there might be some axial chromatic aberration, which means that the focal points of the microscope objective are different between the laser and fluorescence. Therefore, axial chromatic aberration correction is necessary, which can also be achieved by the collimating lens.

Besides, the defocus (Z4), as a special aberration, needs to be considered carefully. The defocus of the microscope objective is precisely what the autofocus system should detect and correct, while the defocus of the collimating lens is the system error decreasing the autofocus working range or even disabling the system. The defocus can be divided into position defocus and temperature defocus. The former can be removed by assembly adjustment, while the

Optics EXPRESS

latter is decided by the influence of the temperature of the working environment. Therefore, it is necessary to analyze the temperature adaptation.

5. Temperature adaptation analysis

The working environment of DNA sequencing might have a small-range temperature fluctuation, usually between 19 °C and 25 °C. Therefore, the microscope with an autofocus system needs to have a certain degree of temperature adaptability. Figure 7 shows the autofocus-microscope operation block diagram. The motor-driven objective moves along the z-axis to compensate for the defocus.

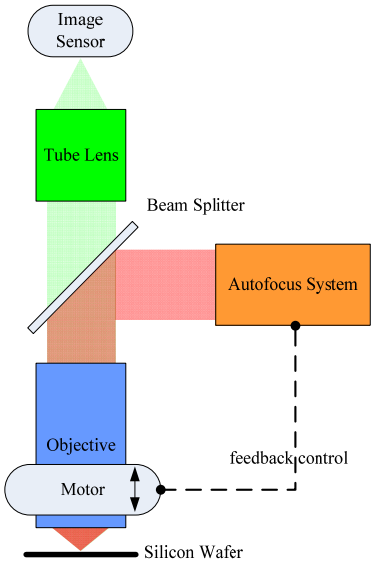

Fig. 7. Block diagram of the autofocus microscope operation.

For the microscope with an autofocus system shown in Fig. 7, a temperature variation can change the focal plane of the objective and the collimating lens. Because the objective focuses the laser for probing the focus and the fluorescence at the same time, temperature affects them in the same manner. On the other hand, the collimating lens of the autofocus system only collimates the laser that might affect the temperature adaptability. Figure 8 shows the change in the focal point position of the collimating lens with temperature. When the temperature deviates from the designated value, PD 1 and PD 2 might lose the symmetry of the position before and after the focus of the collimating lens, which leads to an error in the autofocus.

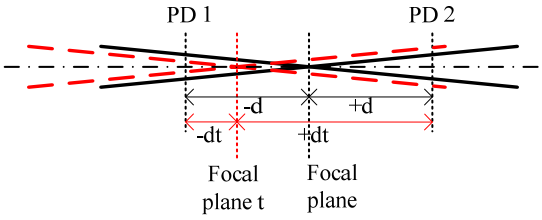

Fig. 8. Variation in the focal point position of the collimating lens with temperature.

Figure 9 shows a doublet collimating lens composed of BK7 glass and F2 glass with a focal length of 60 mm and an aperture of F/4 (SMF NA = 0.12) designed for the autofocus system. The offset of the PDs with pinholes is ± 45 μm calculated from Eq. (3), and the radius

Optics EXPRESS

of the pinholes should be less than 2.16 μm calculated from Eq. (4). When the silicon wafer is in the focal plane of the objective, the normalized differential confocal signal between PD 1 and PD 2 should be zero.

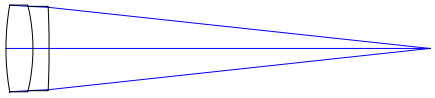

Fig. 9. Layout of the collimating lens.

The lens and the PDs are supported by a tube structure. Temperature adaptation analysis of the collimating tube by ZEMAX software considering optomechanical structure and material properties in a thermal immersion condition shows obvious temperature defocus differences for different tube materials due to the significant difference in the expansion coefficient between aluminum and Invar. Temperature defocus will cause the offset of PD 1 and PD 2 to change, as shown in Fig. 8. Figure 10 shows the offset change with temperature variation.

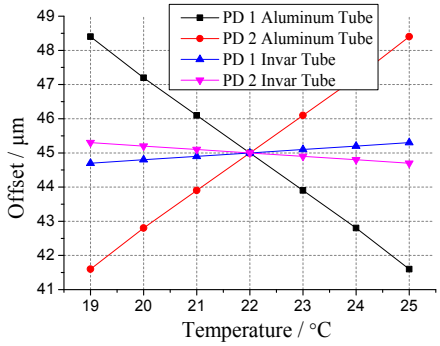

Fig. 10. Offset change with temperature variation.

Then the normalized differential confocal signal in the focal point can be calculated from Eq. (1). Figure 11 shows the differential confocal signal departure from zero with temperature variation. The collimating lens with the aluminum tube induces a departure of ± 0.1 from zero with a temperature variation of ± 3 °C, which represents 0.05 μm autofocus error for an objective with NA = 0.75, which is too large to be acceptable. Using an Invar tube can significantly decrease the temperature sensitivity, which induces a departure of ± 0.01 from zero with the same temperature variation. The corresponding autofocus error is 0.01 μm, which is much better than the required autofocus accuracy.

Optics EXPRESS

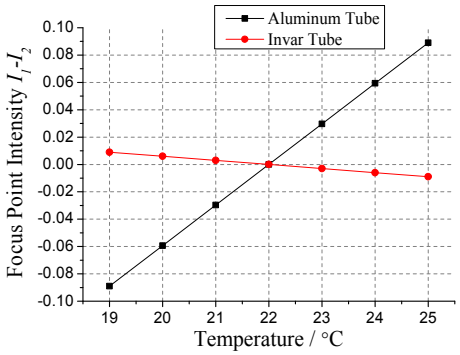

Fig. 11. Departure of the differential confocal signal from zero with temperature variation.

For achieving high autofocus accuracy, the collimating lens needs an athermal design. Here, a collimating lens with an Invar tube is used. For higher accuracy, more sophisticated methods should be applied.

6. Conclusion

This paper presents an autofocus method for a DNA sequencing microscope. High focusing accuracy is achieved using the laser differential confocal technology. Moreover, a new multi-position laser differential confocal method is proposed to expand the autofocus working range. The analysis of degrading effects of optical system aberrations on the autofocus shows that aberration compensation and athermalization are needed to reduce spherical aberration, coma, astigmatism, and defocus. An athermal collimating lens has been designed to cater for the temperature variation between 19 °C and 25 °C for the DNA sequencing environment. Future work will focus on the development of the optical instrument.